

Design and Simulation of Bimorph Piezoactuated Micro Blower

KonduruVenkata Gopinadh¹, P. Mariya Kumar¹, K. Velmurugan²

Department of Mechanical Engineering, V.N.R. College of Engineering, Chintalapudi, Ponnur, Guntur, Andhra Pradesh, India¹
Scientist 'F', Head PETF, ENTEST, RCI, DRDO, Hyderabad, Telangana, India²

ABSTRACT

Advances in the field of avionics have resulted in a significant increase in density Integration, clock rates, and emerging trend of miniaturization of modern electronics. This resulted in dissipation of high heat flux at the chip level. In order to satisfy the junction temperature requirements in terms of performance and reliability, improvements in cooling technologies is required. As a result thermal management is becoming important and increasingly critical to the avionics industry. The task of maintaining acceptable junction temperature by dissipating the heat from the integrated circuit chips is a significant challenge to the thermal engineers. Air cooling is the simplest and principal method of thermal control of avionic systems. Low-power electronic systems are conveniently cooled by natural convection and radiation. When natural convection is not adequate, the forced convection is adopted by a fan or blower to blow the air through the enclosure that houses the avionic components. But, most of the avionic systems must be air tight or sealed, to survive harsh environment, shock load, high vibration, acoustics and EMI/EMC problems. Along with the above concerns, the issue of weight adds to the complexities of thermal management. To overcome above problems, a piezoelectric micro blower, which have large air discharge, has to be designed. This micro blower is an ultra-compact piezoelectric device that is thin enough to be installed in the gaps found in densely packed avionics and develops a high enough pressure to generate sufficient flow rate. The project work deals with the design and analysis of a piezoelectric micro blower. CFD is performed for the flow analysis of a blower.

Keywords: Bimorph Piezoactuated, EMI/EMC, CFD, Integrated Circuits, LSI, CFD, PZT, ALE

I. INTRODUCTION

The field of electronics deals with the construction and utilization of devices that involve current flow through a vacuum, a gas, or a semiconductor. This exciting field of science and engineering dates back to 1883, when Thomas-Edison invented the vacuum diode. The **vacuum tube** served as the foundation of the electronics industry until the 1950s, and played a central role in the development of radio, TV, radar, and the digital computer. Of the several Computers developed in this era, the largest and best known is the ENIAC (Electronic Numerical Integrator and Computer), which was built at the University of Pennsylvania in 1946. It had over 18,000 vacuum tubes and occupied a room 7 m *14 m in size. It consumed a large amount of power, and its reliability was poor because of the high failure rate of the vacuum tubes.

The invention of the bipolar **transistor** in 1948 marked the beginning of a new era in the electronics industry and the obsolescence of vacuum tube technology. Transistor circuits performed the functions of the vacuum tubes with greater reliability, while occupying negligible space and consuming negligible power compared with vacuum tubes. The first transistors were made from germanium, which could not function properly at temperatures above 100°C. Soon they were replaced by silicon transistors, which could operate at much higher temperatures.

The next turning point in electronics occurred in 1959 with the introduction of the **integrated circuits (IC)**, where several components such as diodes, transistors, resistors, and capacitors are placed in a single chip. The number of components packed in a single chip has been increasing steadily since then at an amazing rate, as

shown in Fig.1. The continued miniaturization of electronic components has resulted in *medium-scale integration* (MSI) in the 1960s with 50 to 1000 components per chip, *large-scale integration* (LSI) in the 1970s with 1000 to 100,000 components per chip, and *very large-scale integration* (VLSI) in the 1980s with 100,000 to 10,000,000 components per chip. Today it is not unusual to have a chip 3 cm * 3 cm in size with several million components on it.

The development of the **microprocessor** in the early 1970s by the Intel Corporation marked yet another beginning in the electronics industry. The accompanying rapid development of large-capacity memory chips in this decade made it possible to introduce capable personal computers for use at work or at home at an affordable price. Electronics has made its way into practically everything from watches to household appliances to automobiles. Today it is difficult to imagine a new product that does not involve any electronic parts.

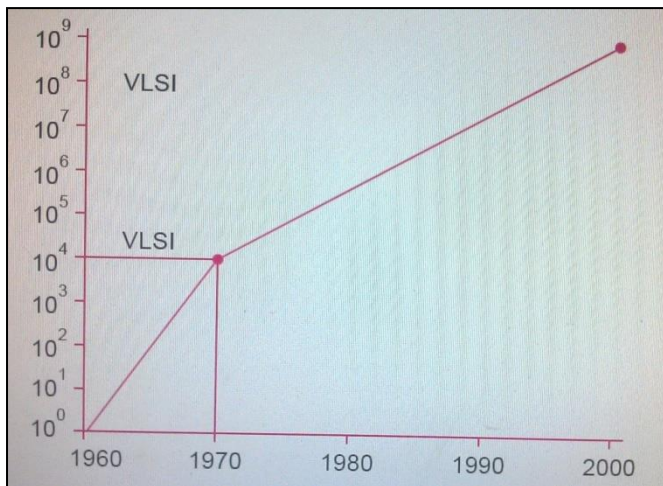


Figure 1.1: The increase in the number of components packed on a chip over the years

The current flow through a resistance is always accompanied by *heat generation* in the amount of I^2R , where I is the electric current and R is the resistance. When the transistor was first introduced, it was touted in the newspapers as a device that “produces no heat.” This certainly was a fair statement, considering the huge amount of heat generated by vacuum tubes. Obviously, the little heat generated in the transistor was no match to that generated in its predecessor. But when thousands or even millions of such components are packed in a small volume, the heat generated increases to such high levels that its removal becomes a

formidable task and a major concern for the safety and reliability of the electronic devices. The heat fluxes encountered in electronic devices range from less than 1 W/cm² to more than 100 W/cm². Heat is generated in a resistive element for as long as current continues to flow through it. In general, a vehicle re-entering the Earth’s atmosphere will have the highest heat flux on its surface. Figure 2 shows the heat flux variation with comparative technologies trend. VLSI electronics heat flux can be comparable with that of re-entry heat flux; this heat flux is very high. Thermal management must be provided for these electronics.

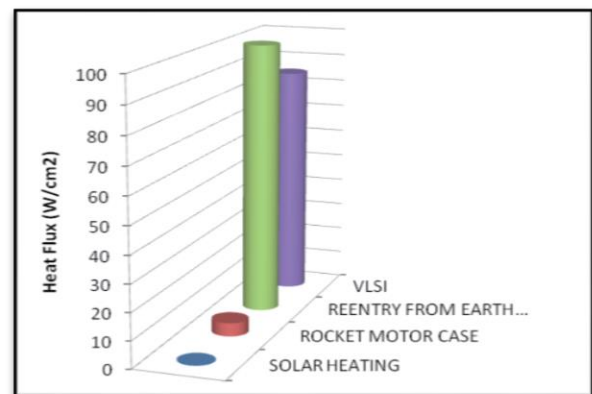


Figure 1.2 : Heat flux vs. comparative technologies trend

Heat is generated in a resistive element for as long as current continues to flow through it. This creates a *heat build-up* and a subsequent *temperature rise* at and around the component. The temperature of the component will continue rising until the component is destroyed unless heat is transferred away from it. The temperature of the component will remain constant when the rate of heat removal from it equals the rate of heat generation. Individual electronic components have *no moving parts*, and thus nothing to wear out with time. Therefore, they are inherently reliable, and it seems as if they can operate safely for many years. Indeed, this would be the case if components operated at room temperature. But electronic components are observed to fail under prolonged use at high temperatures. Possible causes of failure are *diffusion* in semiconductor materials, *chemical reactions*, and *creep* in the bonding materials, among other things. The failure rate of electronic devices increases almost *exponentially* with the operating temperature, as shown in Figure 3. The cooler the electronic device operates, the more reliable it is. A rule of thumb is that the failure rate of electronic

components is halved for each 10°C reduction in their junction temperature.

From a reliability and performance point of view, thermal management needs to be carried out for every electronic device which dissipates heat. This is essential for modern electronics, for as they consume more power, they also generate more heat. This has led to the development of computational fluid dynamics (CFD) simulation software and advances in thermal management techniques. The increasing complexity and power density of modern electronics has challenged the traditional approach of using prototypes and testing. The modern CFD simulation software developed for challenging environments and high power dissipation devices has led to a reduction in the product development cycle.

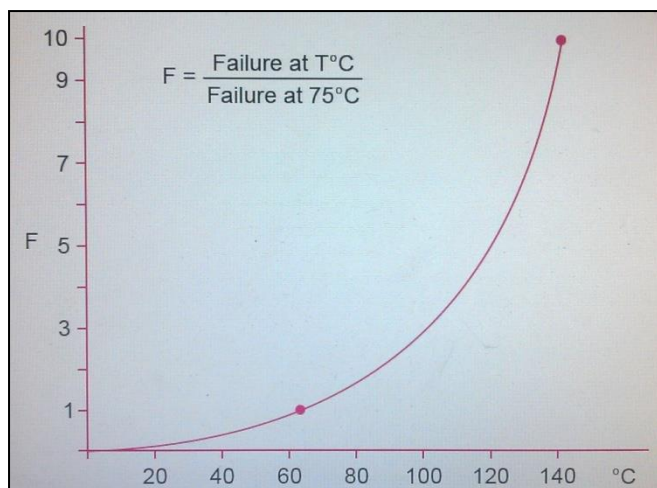


Figure 1.3 : The increase in the failure rate of bipolar digital devices with temperature

II. METHODS AND MATERIAL

The work deals with the study the fluid characterization of the piezoelectric micro blower. CFD is performed for the flow analysis of piezoelectric micro blower using COMSOL MULTIPHYSICS simulation software. The results of flow analysis are used to study the thermal characteristic of a piezoelectric micro blower for cooling a hot component. An attempt is also made to study the effect of the load i.e. voltage applied, frequency and the orifice diameter on the performance of piezoelectric micro blower.

The piezoelectric micro blower designed in this project consists of single actuator plate, which is operated by sinusoidal voltage. The piezoelectric micro blower is

modelled in SOLIDWORKS software and the flow analysis is carried out using the CFD commercial software COMSOL MULTIPHYSICS. The medium used in this analysis is air. The velocity distribution and mass flow rate of the piezoelectric micro blower are observed.

The first objective is the selection of piezoelectric actuator material for the fixed outer dimensions of micro blower. Once the modal, transient-structural and previously mentioned values are decided, CFD analysis of the piezoelectric micro blower is performed to obtain a better understanding of the piezoelectric micro blower.

- 3D model and 2D drawings of the piezoelectric micro blower is developed by using SOLIDWORKS software.
- Static structural analysis of actuator model is done in COMSOL MULTIPHYSICS simulation software to optimize the actuator dimensions.
- Modal-analysis of actuator model is done in COMSOL MULTIPHYSICS simulation software to know the operating frequency of the actuator.
- Transient-Structural analysis of the actuator is performed in COMSOL MULTIPHYSICS simulation software to study the dynamic displacement and stress.
- Coupled Multiphysics analysis of Transient-structural and Fluid flow is performed in COMSOL MULTIPHYSICS simulation software.

Design & Simulation of Piezoelectric Micro Blower

2.1: Selection of shape and outer dimensions of Piezoelectric Micro blower:

The outer shape and outer dimensions of piezoelectric micro blower depend upon the mounting space available for the micro blower in avionics package. Generally commercial piezoelectric micro blower outer shape is square with outer dimensions of 20mm×20mm×2mm. Thus the mounting are required for those types of blowers are area of the base of that blower. Here we are going to design a circular piezoelectric micro blower of diameter 35mm. These circular piezoelectric micro blowers need less mounting area on compared to the regular commercial micro blowers. The height of the micro blower is selected based upon the transient

structural analysis. The actuator plate, top plate, flow path plate, separator plate, blower chamber plate, and bottom plate will have the same circular outer shape of diameter 35mm.

2.2: Selection of Type of actuator diaphragm dependent upon the type of arrangement of piezoelectric materials:

The diaphragm of the present project may be any one of the following types:

Unimorph: A unimorph diaphragm formed by attaching a piezoelectric element to one surface of a resin plate or a metal plate, the piezoelectric element expanding and contracting in a planer direction.

Bimorph: A bimorph diaphragm formed by attaching piezoelectric elements to both surfaces of a resin plate or a metal plate, the piezoelectric elements each expanding and contracting in a direction opposite that of the other piezoelectric element.

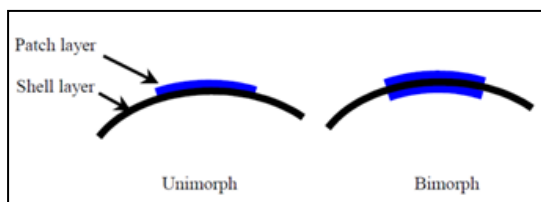


Figure 2.1: Unimorph and Bimorph arrangement

Multilayer bimorph: A bimorph diaphragm formed by attaching a multilayer piezoelectric element to one surface of a resin plate or a metal plate, the multilayer piezoelectric element being capable of bending itself; and a diaphragm entirely composed of a multilayer piezoelectric element. [10]

For the present project, Multilayer bimorph is not suitable. If we use multi-layered bimorph it results in the increase in the height of the actuator. Thus results in the more chamber height, which automatically results in the increase of the height of piezoelectric micro blower. The diaphragm of the present project is may be any of the unimorph and bimorph. The selection in between unimorph and bimorph is decided by the static structural analysis done in COMSOL multi physics simulation software. [7]

Materials used for this Static structural analysis are as follows:

Actuator plate: Aluminium plate of 30mm diameter and 100 μ m thickness

Piezoelectric plate: Circular PZT-5H of 20mmdiameter and thickness of 100 μ m

2.3: selection of material for actuator diaphragm:

2.3.1: Selection of material for piezoelectric plates:

Recently, several piezoelectric materials, Lead Titanate Zirconate Ceramics (PZT-4, PZT-5A, PZT-5H, and PZT-7A etc.), Barium Titanate, and Poly vinylidene Fluoride are invented and characterized. The piezoelectric material should have high d_{31} & d_{33} values to get maximum deflection in direction of polarization as well as in the radial direction. Among all the above mentioned piezoelectric materials PZT-5H has the high d_{31} & d_{33} values. And also The PZT-5H ceramics exhibited the largest piezoelectric coefficients at room temperature. PZT-5H exhibited the largest piezoelectric properties up to its Curie point (170 $^{\circ}$ C). This PZT-5H material possess properties that are suitable for use in some aerospace applications. Because of all these reason we are selecting PZT-5H as piezoelectric material for this project. [10]

Piezo Mat (PIEZ) Table For Material 1 Piezoelectric strain matrix [d]	<table border="1"> <thead> <tr> <th colspan="2"></th> <th colspan="2">X</th> </tr> <tr> <th>Y</th> <th>Z</th> <th></th> <th></th> </tr> </thead> <tbody> <tr> <td>X</td> <td></td> <td>0.0000</td> <td></td> </tr> <tr> <td></td> <td></td> <td>0.22000E-10</td> <td></td> </tr> <tr> <td></td> <td></td> <td>0.0000</td> <td></td> </tr> <tr> <td>Y</td> <td>0.0000</td> <td>-</td> <td></td> </tr> <tr> <td></td> <td></td> <td>0.30000E-10</td> <td></td> </tr> <tr> <td></td> <td></td> <td>0.0000</td> <td></td> </tr> <tr> <td>Z</td> <td></td> <td>0.0000</td> <td></td> </tr> <tr> <td></td> <td></td> <td>0.30000E-11</td> <td></td> </tr> <tr> <td></td> <td></td> <td>0.0000</td> <td></td> </tr> </tbody> </table>			X		Y	Z			X		0.0000				0.22000E-10				0.0000		Y	0.0000	-				0.30000E-10				0.0000		Z		0.0000				0.30000E-11				0.0000	
		X																																											
Y	Z																																												
X		0.0000																																											
		0.22000E-10																																											
		0.0000																																											
Y	0.0000	-																																											
		0.30000E-10																																											
		0.0000																																											
Z		0.0000																																											
		0.30000E-11																																											
		0.0000																																											
Piezoelectric stress matrix [e] computed from the piezoelectric strain matrix [d] and anisotropic elasticity matrix	<table border="1"> <thead> <tr> <th colspan="2"></th> <th colspan="2">X</th> </tr> <tr> <th>Y</th> <th>Z</th> <th></th> <th></th> </tr> </thead> <tbody> <tr> <td>X</td> <td></td> <td>0.0000</td> <td></td> </tr> <tr> <td></td> <td></td> <td>0.28756E-01</td> <td></td> </tr> <tr> <td></td> <td></td> <td>0.0000</td> <td></td> </tr> <tr> <td>Y</td> <td>0.0000</td> <td>-</td> <td></td> </tr> <tr> <td></td> <td></td> <td>0.51864E-01</td> <td></td> </tr> <tr> <td></td> <td></td> <td>0.0000</td> <td></td> </tr> <tr> <td>Z</td> <td>0.0000</td> <td>-</td> <td></td> </tr> <tr> <td></td> <td></td> <td>0.70137E-03</td> <td></td> </tr> <tr> <td></td> <td></td> <td>0.0000</td> <td></td> </tr> </tbody> </table>			X		Y	Z			X		0.0000				0.28756E-01				0.0000		Y	0.0000	-				0.51864E-01				0.0000		Z	0.0000	-				0.70137E-03				0.0000	
		X																																											
Y	Z																																												
X		0.0000																																											
		0.28756E-01																																											
		0.0000																																											
Y	0.0000	-																																											
		0.51864E-01																																											
		0.0000																																											
Z	0.0000	-																																											
		0.70137E-03																																											
		0.0000																																											
D Matrix	<table border="1"> <tbody> <tr> <td>D11</td> <td>0.50000E-09</td> </tr> <tr> <td>D12</td> <td>-0.14500E-9</td> </tr> <tr> <td>D13</td> <td>-0.14500E-9</td> </tr> <tr> <td>D22</td> <td>0.50000E-9</td> </tr> <tr> <td>D23</td> <td>-0.14500E-9</td> </tr> <tr> <td>D33</td> <td>0.50000E-9</td> </tr> </tbody> </table>	D11	0.50000E-09	D12	-0.14500E-9	D13	-0.14500E-9	D22	0.50000E-9	D23	-0.14500E-9	D33	0.50000E-9																																
D11	0.50000E-09																																												
D12	-0.14500E-9																																												
D13	-0.14500E-9																																												
D22	0.50000E-9																																												
D23	-0.14500E-9																																												
D33	0.50000E-9																																												

	D44 0.12903E-08
Dielectric Permittivity, at constant stress	EP11 12.000 EP22 12.000
Piezoelectricity e (cm-2)	0.0 0.0 -5.4 0.0 0.0 -5.4 0.0 0.0 15.8 0.0 0.0 0.0 0.0 12.3 0.0 12.3 0.0 0.0
Permittivity ϵ (F m-1) $\times 10^{-9}$	8.107 0 0 0 8.107 0 0 0 7.346
Compliance S (m2 N-1) $\times 10^{-12}$	16.4 -5.75 -8.45 0 0 0 0 16.4 -8.45 0 0 0 0 0 0 Symmetry 44.3 0 0 47.5 0 47.5
Density (Kgm-3)	7500
Poison's ratio	0.3
Young's modulus E (GPa)	126

Table 2.1 Material Properties for Two Dimensional Bimorph PZT-5H

2.3.2: Selection of material for vibrating plate:

A vibrating plate should have low stiffness to bend and high strength to withstand for the vibrations caused by the piezo actuation. Here we are going to select the material of vibrating plate by the results of static structural analysis done in COMSOL multi physics simulation software for different materials. [1]

For this simulation bimorphpiezo arrangement is used. The vibrating plate of diameter 30mm and thickness of 100 μ m is used. Piezo electric material, PZT-5H of diameter 30mm and thickness of 100 μ m is used. Material of vibrating plate is varied as Aluminium, Copper, Iron, Nickel, Silica Glass, Silicon and Steel.

2.3.3: Selection of thickness of vibrating plate and piezoelectric plate:

The thickness of the vibrating plate and piezoelectric material should be very small. As the thickness of these plates increases the stiffness also increases. Then plate

vibrates with smaller deflections. So, we are taking vibrating plate thickness as 100 μ m.

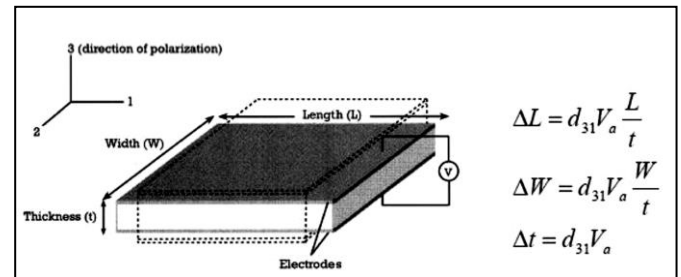


Figure 2.2: The deformation and simply equations of the piezoelectric material

The strain developed by the piezoelectric material depends upon the Voltage applied across the electrodes. In our case direction of polarization of beam is in the direction of d_{31} i.e. along the thickness direction.

Change in thickness of piezo on application of V_a voltage across the thickness is given by the formula

$$\Delta t = d_{31} \cdot V_a \quad (4.1)$$

The strain developed in the piezoelectric plate along thickness is given by,

$$e_t = \frac{\Delta t}{t} = \frac{d_{31}}{t} \cdot V_a \quad (4.2)$$

When these piezos are attached to the vibrating plate, the strain developed by the piezos is equal to the strain acted upon the vibrating plate. Thus deformation occurs in plate. To get the maximum strain in the vibrating plate the thickness of piezoelectric material should be very small. For this project we are taking a piezoelectric thickness of 100 μ m. By using above mentioned parameters the actuator plate is designed.

2.4: Model analysis of actuator:

Modal analysis is the study of the dynamic properties of structures under vibrational excitation. The goal of modal analysis in structural mechanics is to determine the natural mode shapes and frequencies of an object or structure during free vibration.[2]

To solve this analysis the boundary conditions and mesh formed are shown below. The diaphragm plate is fixed at edges and voltage is not applied across the piezoelectric materials

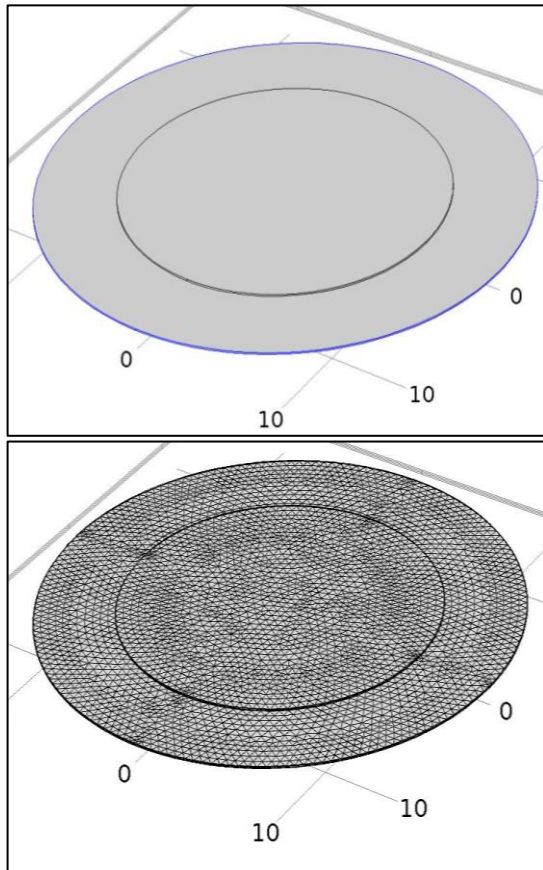


Figure 2.3: Bimorph Piezo actuator with fixed constraints at edges and mesh applied

2.5 Transient structural analysis of actuator:

This analysis is done to optimize the total deformation and the stress generated by the actuator plate due to the AC voltage. By this analysis we can finalize the height of blower chamber and thickness of bottom plate of piezoelectric actuator. The average deflection of the actuator is taken as the height of the blower chamber.

Boundary condition: Ends of the actuator (plate) is fixed. Hence the displacements and rotation in all the three directions are restrained to simulate. Transient analysis is run for 20 cycles.

Voltage: For the analysis the plate is meshed using a shell element, and then the boundary condition is applied. Then the applied load is defined using the option 'function' in the definitions and it is assumed that applied voltage has no phase difference.

The voltage is given in the form of sinusoidal wave as

$$V = V_0 * \sin(2 * \Pi * f * t) \text{ in Volts} \quad (4.3)$$

Where, f= frequency of vibration of the plate

$$V_0 = 14 V_{p-p}$$

Time = variable in seconds

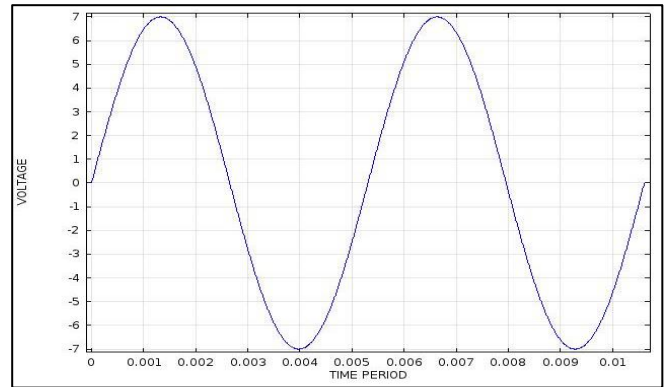


Figure 2.4: Sinusoidal input for transient structural analysis

From the results the maximum displacement of the actuator is found to be 22µm peak to peak. So, we are taking the blower chamber height as 1.75mm. The thickness of the bottom plate should be greater than the average displacement of actuator and thickness of piezoelectric patch, so it is taken as 2mm.

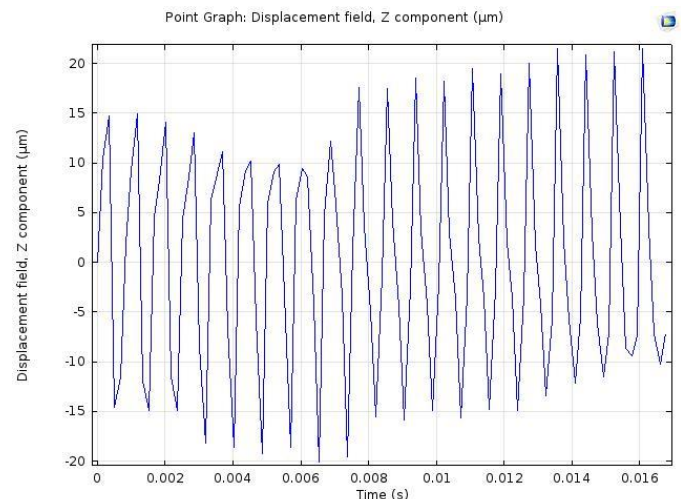


Figure 2.5: Displacement of actuator in Z-direction in transient analysis

Separator plate is designed with a diameter of 30mm and thickness of 0.1mm. The hole at the centre of the separator plate serves as a first opening. The diameter of first opening is taken as 0.6mm. The flow path plate thickness is taken as 0.4mm to create a clear path for the incoming flow in to the blower chamber. The top plate thickness is taken as 0.35mm for this project. The outlet which is at the centre of top plate and in axis with the first opening diameter is taken as of 0.8mm. A nozzle of height 2mm is designed. All are designed using SOLIDWORKS design software.

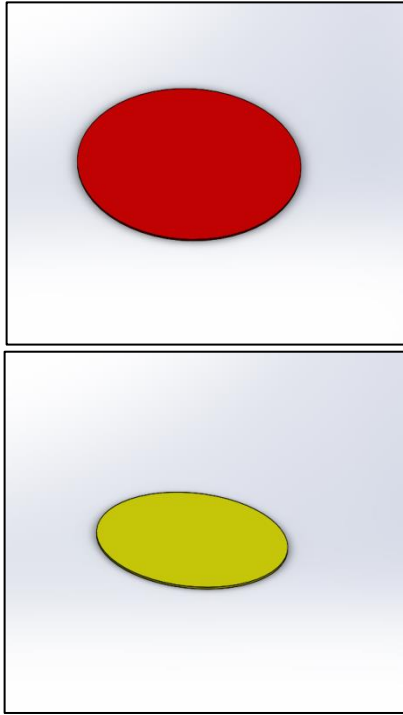


Figure 2.6: (a)Vibrating plate; (b) PZT

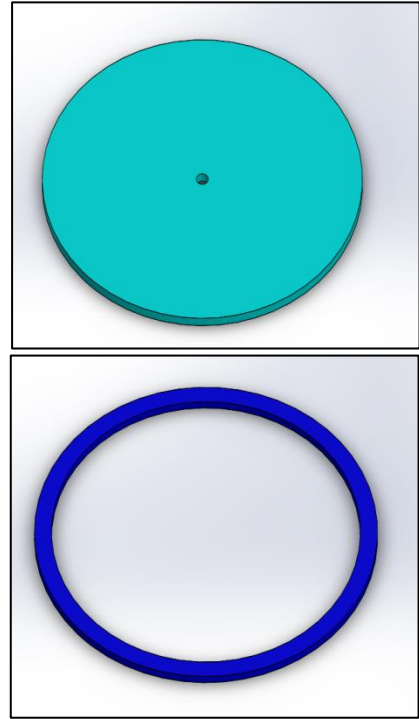


Figure 2.8: (a) Top Plate; (b) Blower Chamber



Figure 2.7: (a) Assembly of Vibrating Plate + PZT;
(b)Separator Plate

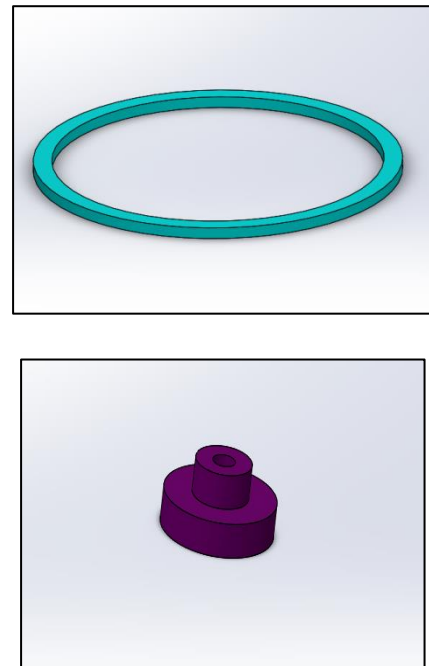
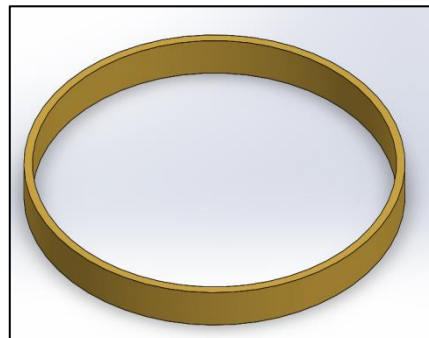


Figure 2.9: (a) bottom plate; (b)Nozzle



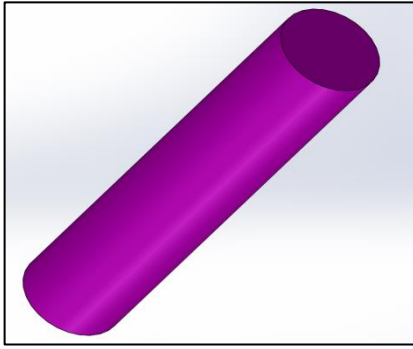


Figure 2.10: (a)Side cover; (b) Pin on which connects separator and top plate

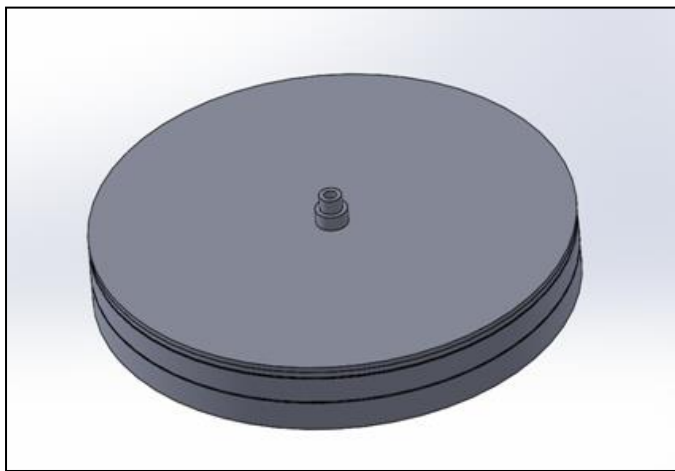


Figure 2.11: Final assembly of piezoelectric micro blower

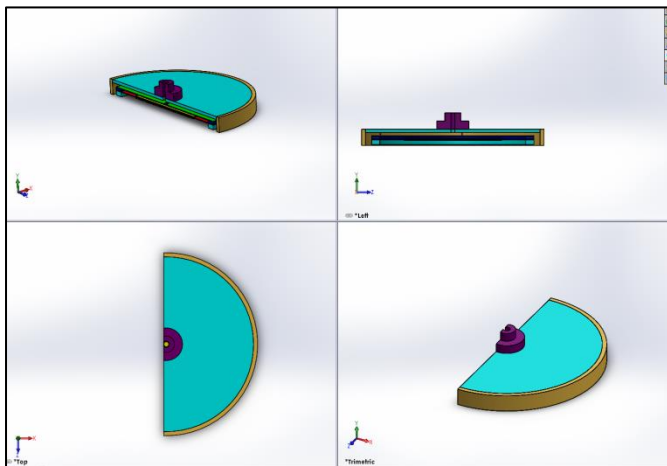


Figure 2.12: section view of micro blower

2.12 Transient Fluid-structural Flow Analysis CFD Based

Mathematical modelling of a continuum problem leads to a set of differential, integral or integral-differential equations. Exact analytical solution of such equations is limited to problems in simple geometries. Hence, for most of the problems of practical interest, an

approximate numerical solution is sought. In the context of mechanics, the science and practice of obtaining approximate numerical solution using digital computers is termed computational mechanics. For thermo-fluid problems, this approach is popularly known as computational fluid dynamics (CFD). Thus, note that although word heat transfer is missing from CFD, it is an intrinsic part of this discipline. CFD deals with approximate numerical solution of governing equations based on the fundamental conservation laws of physics, namely mass, momentum and energy conservation. The CFD solution involves

- Conversion of the governing equations for a continuum medium into a set of discrete algebraic equations using a process called discretization.
- Solution of the discrete equations using a high speed digital computer to obtain the numerical solution to desired level of accuracy.

Computational fluid dynamics (CFD) has become an essential tool in analysis and design of thermal and fluid flow systems in wide range of industries. Few prominent areas of applications of CFD include meteorology, transport systems (aerospace, automobile, high-speed trains), energy systems, environment, electronics, bio-medical (design of life support and drug delivery systems), etc. Component designers and systems architects are increasingly turning to electronic design automation (eda) to reap cost saving and timesaving benefits.

Fluid – Structural Interaction Problem:

The Multiphysics iteration between the bimorph piezoelectric actuator, which deforms due to the alternating voltage and the fluid, COMSOL Multiphysics a suitable tool for the computational analysis of the bimorph piezoelectric micro blower. For this analysis, the axisymmetric model wizard was selected in COMSOL multiphysics. The entire micro blower is converted in to 2D axisymmetric model and Incompressible laminar flow and moving mesh (ALE) were used.

Steps for the Multiphysics Analysis:

In modal wizard select 2D axisymmetric model. In multiphysics selection, select piezoelectric device from solid mechanics, Moving mesh (ALE) under

Mathematics>Deformed Mesh and Laminar flow(spf) interface, found under the Single-Phase Flow branch in flow analysis.

The Solid Mechanics (solid) interface, found under the Structural Mechanics branch when adding a physics interface, is intended for general structural analysis of 3D, 2D, or axisymmetric bodies. In 2D, plane stress or plane strain assumptions can be used. The Solid Mechanics interface is based on solving Navier's equations, and results such as displacements, stresses, and strains are computed. [8]

The Moving Mesh (ale) interface, found under the Mathematics>Deformed Mesh branch when adding a physics interface, can be used to create models where the geometry, here represented by the mesh, changes shape due to some physical phenomena without material being removed or added. The difference between the Deformed Geometry and Moving Mesh interfaces is that the former defines a deformation of the material frame relative to the geometry frame, while the latter defines a displacement of the spatial frame relative to the material frame. The Moving Mesh interface can be used to study both stationary states and time-dependent deformations where the geometry changes its shape due to the dynamics of the problem.

The Laminar Flow (spf) interface, found under the Single-Phase Flow branch when adding a physics interface, is used to compute the velocity and pressure fields for the flow of a single-phase fluid in the laminar flow regime. A flow remains laminar as long as the Reynolds number is below a certain critical value.

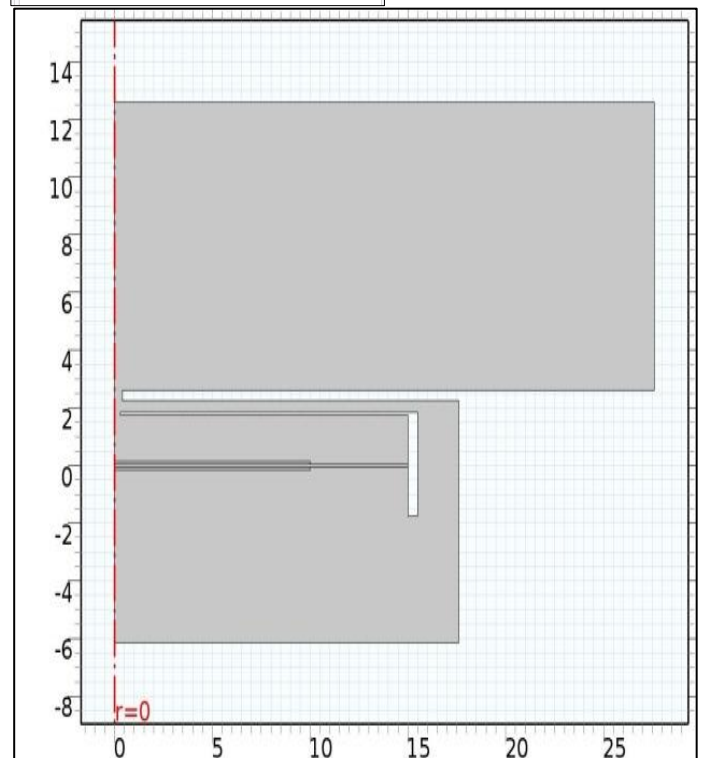
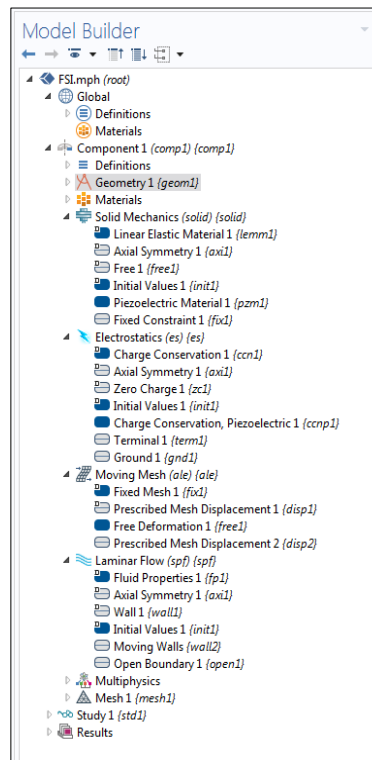


Figure 2.13:The model Builder and Fluid domain and actuator design in 2D

Governing Equations:

The 2nd order partial differential equations which govern the conservation of mass, momentum for three dimensional flow (laminar or turbulent) are written. The fluid is assumed to be incompressible.

These equations are expressed as follows:

- Conservation of mass

$$\nabla \cdot \mathbf{V} = 0$$

$$\frac{\partial u}{\partial x} + \frac{\partial v}{\partial y} + \frac{\partial w}{\partial z} = 0$$

- Conservation of momentum

$$\frac{D\mathbf{V}}{Dt} = \frac{\partial \mathbf{V}}{\partial t} + (\mathbf{V} \cdot \nabla)\mathbf{V} = -\frac{1}{\rho} \nabla P + \nu \nabla^2 \mathbf{V}$$

$$\frac{\partial u}{\partial t} + u \frac{\partial u}{\partial x} + v \frac{\partial u}{\partial y} + w \frac{\partial u}{\partial z} = -\frac{1}{\rho} \frac{\partial P}{\partial x} + \nu \left(\frac{\partial^2 u}{\partial x^2} + \frac{\partial^2 u}{\partial y^2} + \frac{\partial^2 u}{\partial z^2} \right)$$

$$\frac{\partial v}{\partial t} + u \frac{\partial v}{\partial x} + v \frac{\partial v}{\partial y} + w \frac{\partial v}{\partial z} = -\frac{1}{\rho} \frac{\partial P}{\partial y} + \nu \left(\frac{\partial^2 v}{\partial x^2} + \frac{\partial^2 v}{\partial y^2} + \frac{\partial^2 v}{\partial z^2} \right)$$

$$\frac{\partial w}{\partial t} + u \frac{\partial w}{\partial x} + v \frac{\partial w}{\partial y} + w \frac{\partial w}{\partial z} = -\frac{1}{\rho} \frac{\partial P}{\partial z} + \nu \left(\frac{\partial^2 w}{\partial x^2} + \frac{\partial^2 w}{\partial y^2} + \frac{\partial^2 w}{\partial z^2} \right)$$

Where, ρ is the density (Kg/m^3)

ν is the kinematic viscosity (Kg/m-s)

\mathbf{V} is the velocity field (m/s)

P is the dynamic pressure (Pa)

u, v, w are velocity in $x-, y-, z-$ directions resp. (m/s)

Solid Modelling:

Fixed Constraint: In solid mechanics, the fixed constrain is applied at the edge of the aluminium plate so that the displacement and rotation of it is arrested in all the three directions.

Load Applied: Terminal voltage is applied as a function of sine and at the rate of the solids (Diaphragm) natural frequency.

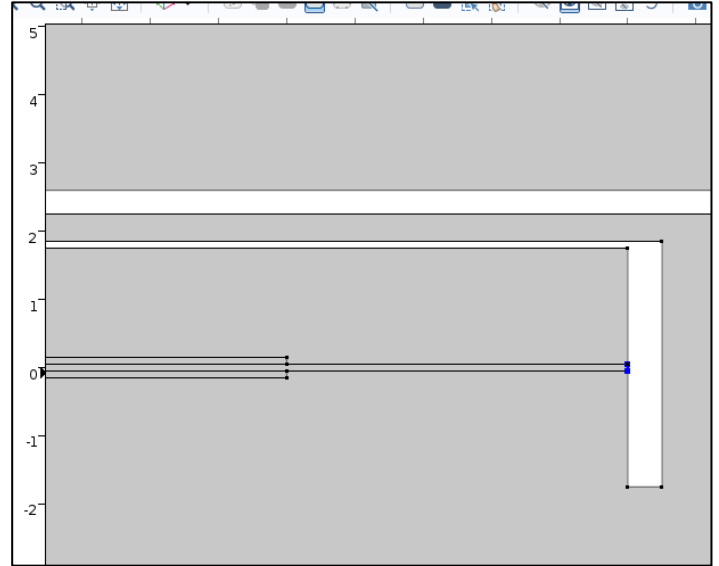


Figure 2.14: In Solid mechanics fixed constrain applied for aluminium plate

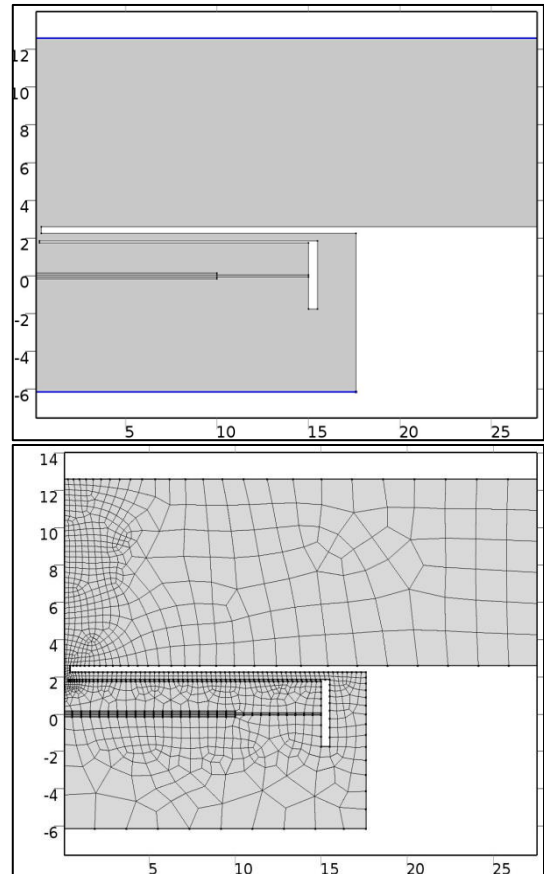
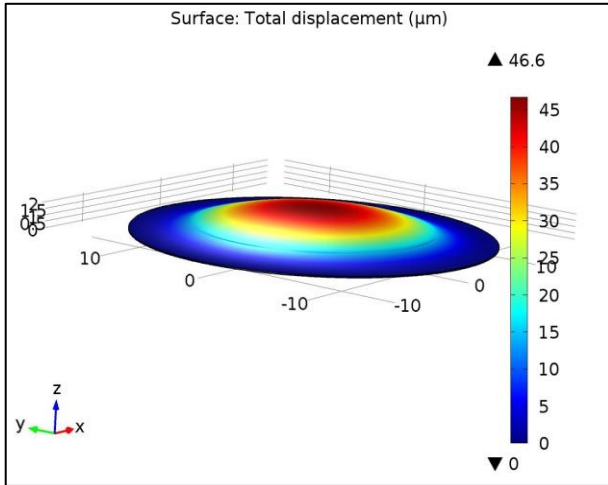


Figure 2.15: Open boundary applied for fluid domain and Mesh applied for entire geometry

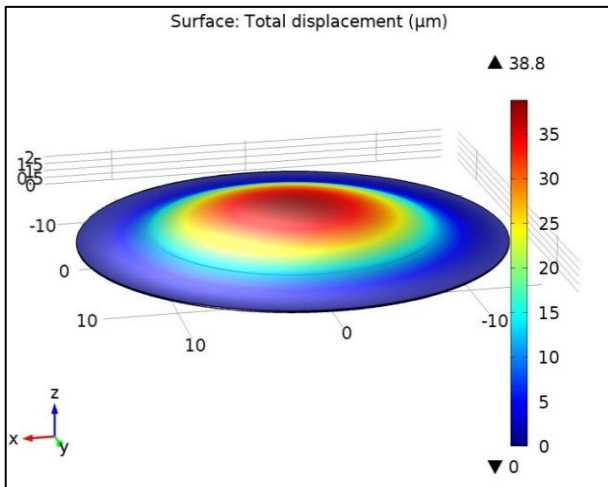
III. RESULTS AND DISCUSSION

(i) Deflection due to Unimorph and Bimorph:

In the case of bimorph piezoelectric arrangement, we get a total deflection of $46.6\mu\text{m}$, and in case of unimorph we are getting a deflection of $38.8\mu\text{m}$ only for the voltage of 30V . By this simulation, we conclude that bimorph arrangement is better than unimorph.



(a)



(b)

Figure 3.1: (a) Deflection due to bimorph piezo actuation, (b) Deflection due to unimorph piezo actuation

(ii) Selection of material for vibrating diaphragm:

From the simulation results we observe that the maximum deflection is obtained for Silica glass of $47\mu\text{m}$ and for Aluminium $46.6\mu\text{m}$ which are nearly equal. For this project we are selecting aluminium as a material for vibrating plate because of its high strength towards vibration and its low weight.

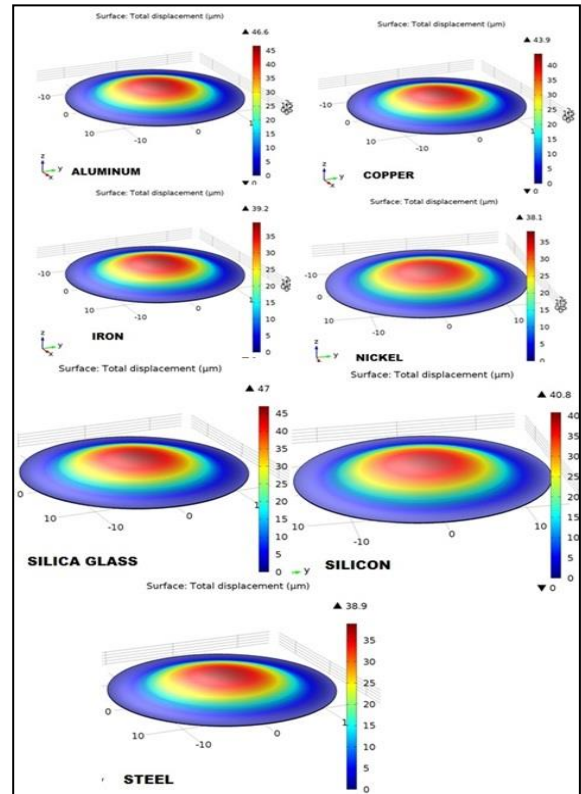


Figure 3.2: Deflections of different materials of bimorph arrangement for 30V

Sl. No	Material	Maximum Deflection in μm
1	Aluminum	46.6
2	Copper	43.9
3	Iron	39.2
4	Nickel	38.1
5	Silica Glass	47
6	Silicon	40.8
7	Steel	38.9

TABLE 3.1 : Deflection of bimorph piezo actuator for different materials of vibrating plate

(iii) Selection of operating frequency of actuator:

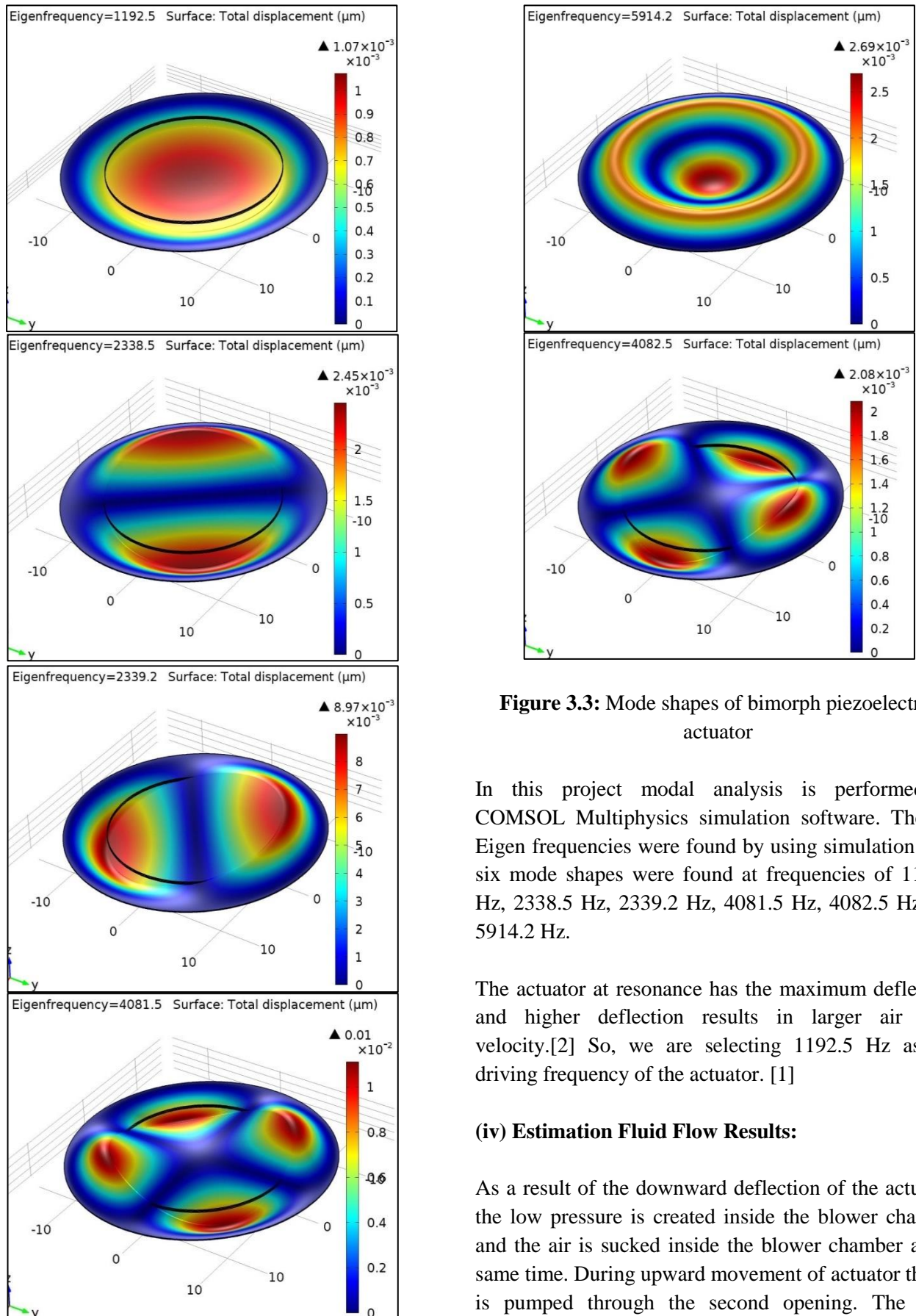


Figure 3.3: Mode shapes of bimorph piezoelectric actuator

In this project modal analysis is performed in COMSOL Multiphysics simulation software. The six Eigen frequencies were found by using simulation. The six mode shapes were found at frequencies of 1192.5 Hz, 2338.5 Hz, 2339.2 Hz, 4081.5 Hz, 4082.5 Hz and 5914.2 Hz.

The actuator at resonance has the maximum deflection and higher deflection results in larger air flow velocity.[2] So, we are selecting 1192.5 Hz as the driving frequency of the actuator. [1]

(iv) Estimation Fluid Flow Results:

As a result of the downward deflection of the actuator, the low pressure is created inside the blower chamber and the air is sucked inside the blower chamber at the same time. During upward movement of actuator the air is pumped through the second opening. The fluid analysis is done for first four cycles. During these cycles, we observe the vertices formation in the fluid domain. [3]

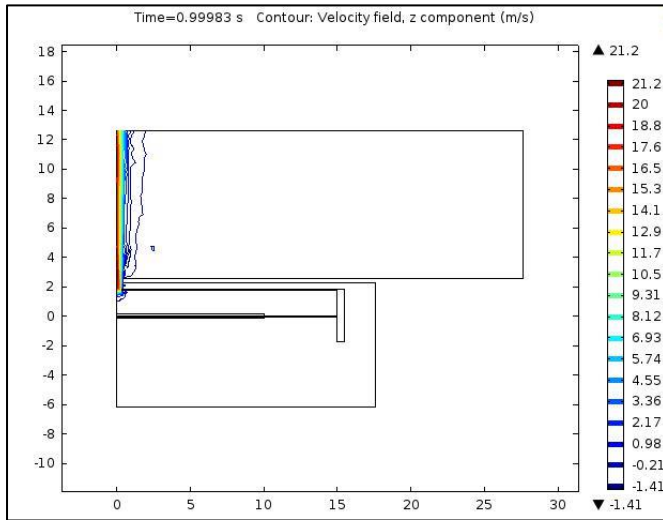


Figure 3.4: Contour plot for velocity field in Z direction

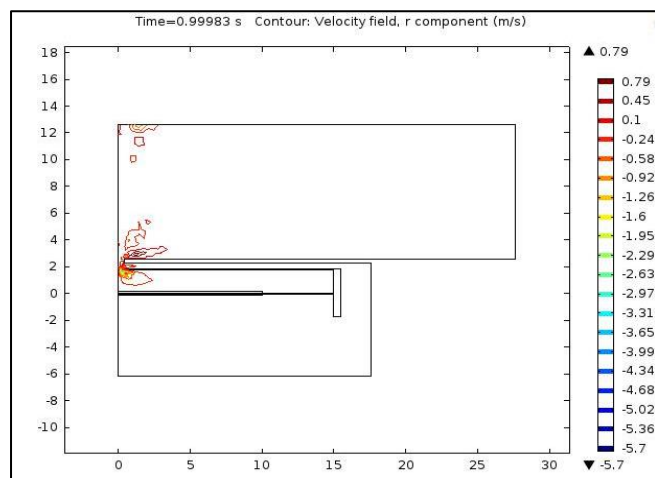


Figure 3.5: Contour plot for velocity field in radial direction with vortices formation

The volume flow rate is calculated by using the formula

$$v = AV$$

Where, m = mass flow rate

ρ = density of air

V = Average velocity of fluid

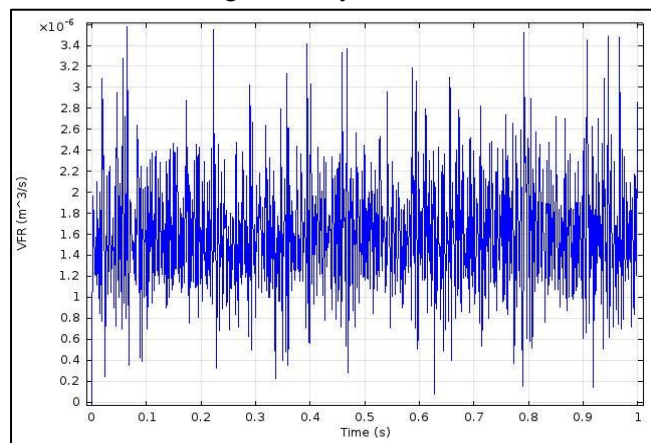


Figure 3.6: Net Volume Flow rate of air from the outlet during every time interval

The net volume flow rate of air across the nozzle outlet is calculated by using the expression of volume flow rate and is obtained as $1.91E-03 \text{ m}^3/\text{s}$. This value of net volume flow rate is more than the volume flow rate of convective available piezoelectric micro blower.

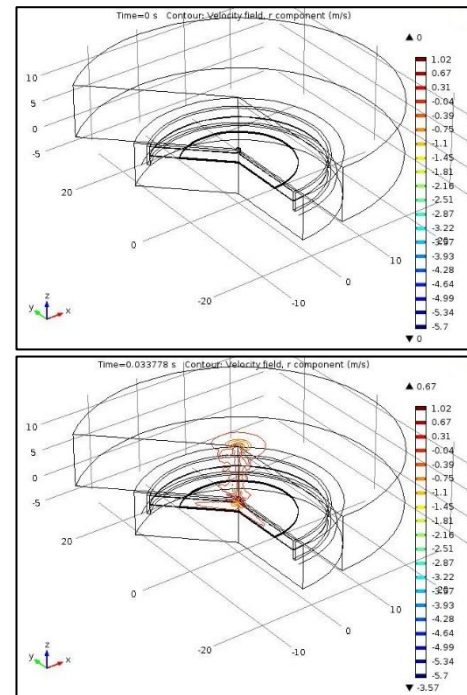


Figure 3.7: Formation of vortices for every time step

IV. CONCLUSION

A clear jet formation is observed from the CFD based fluid structure interaction of the piezoelectric actuated micro blower designed for the thermal management of high power components. Under operating conditions of the micro blower, a vortex ring (a vortex pair in the 3D) is formed at the orifice edge during the expulsion part of the cycle. This vortex ring is convected away from the orifice. Since the self-induced velocity of the vortex ring is strong enough, the vortex pair is not injected back in the orifice during the suction part of the cycle. The formation of vortex ring is defined here in as the onset of jet formation.

V. FUTURE WORK

- Study the influence of the vortex rings interactions with the diaphragm in the quality of jet formation.
- Study of the influence of the actuator's height.
- Study the influence of the stiffness of the actuator in the jet formation.
- Study of the flow phenomena using turbulence model.
- Study the flow phenomenon by varying the outlet diameter.
- Study the flow phenomenon by varying the diameter of first opening.
- Study the flow phenomenon by varying the flow path plate i.e., inlet path

VI. REFERENCES

- [1] Qifeng Cui, Chengliang Liu and Xuan F. (William) Zha, "Design and simulation of a piezo electrically actuated micro pump for the drug delivery system", Proceeding of the 2006 IEEE International Conference on Automation Science and Engineering, Shanghai, China, October 7-10, 2006
- [2] Manoj Pandey and P.C. Upadhyay., "Design and Simulation of Valve Less PZT Micro pump for Drug Delivery System", International Journal of Advancements in Technology, <http://ijict.org/> ISSN 0976-4860, Vol. 3 No.2 (April 2012) © IJoAT
- [3] B Fan, G Song and F Hussain, "Simulation of a piezo electrically actuated Valve less micro pump", Institute Of Physics Publishing Smart Materials And Structures, Smart Mater. Struct. 14 (2005) 400–405 doi:10.1088/0964-1726/14/2/014
- [4] Chiang-Ho Cheng and Chih-Kai Chen, "Characteristic Studies of the Piezo electrically Actuated Valve less Micro pump", Proceedings of the World Congress on Engineering 2013 Vol III, WCE 2013, July 3 - 5, 2013, London, U.K.
- [5] Juan J. Rojas, Jose E. Morales, "Design and Simulation of a Piezoelectric Actuated Valve less Micro pump", Excerpt from the Proceedings of the 2015 COMSOL Conference in Boston
- [6] Michal Staworko and Tadeusz UHL, "Modelling and simulation of piezoelectric elements _ comparison of available methods and tools", Mechanics Vol. 27 No:4, 2008
- [7] Mukesh Tak and Saurab M. Patel, "Determination of tip's deflections of a piezoelectric cantilever beam with voltage variation", 978-1-4799-7678-2/15/\$31.0 ©2015 IEEE
- [8] David C. Duran AND Omar D. Lopez, "Computation Modelling of synthetic jets", excerpt from the proceedings of the COMSOL conference 2010, Boston.
- [9] COMSOL multiphysics manual
- [10] J.W. Wanders, Piezoelectric Ceramics, 1st edition 1991 Eindhoven 4-91
- [11] "Piezoelectric Micro blower", by Murata Manufacturing Co. Ltd.